0270-6474/85/0504-1035$02.00/0

Printed in U.S.A.

The Journal of Neuroscience
Vol. 5, No. 4, pp. 1035–1048
April 1985

Membrane Assembly in Retinal Photoreceptors

III. Distinct Membrane Domains of the Connecting Cilium of Developing Rods[1]

JOSEPH C. BESHARSE,[2] DONNA M. FORESTNER, AND DENNIS M. DEFOE

Department of Anatomy, Emory University School of Medicine, Atlanta, Georgia 30322

Abstract

To investigate the putative role of the photoreceptor connecting cilium in the delivery of opsin to forming discs and in the maintenance of membrane domains (Besharse, J. C., and K. H. Pfenninger (1980) J. Cell Biol. *87:* 451–463), we have studied developing photoreceptors of neonatal rats during the period of initial disc formation using conventional freeze-fracture, immunocytochemistry, and lectin cytochemistry. Specific anti-opsin-binding sites were localized in the distal cilium, the developing outer segment plasma membrane, and at focal sites on the inner segment plasma membrane at all developmental stages examined, including the period prior to the onset of disc morphogenesis. The proximal ciliary shaft generally lacked anti-opsin-binding sites or exhibited them in extremely low density. The distribution of anti-opsin-binding sites corresponded in a general way to the distribution of large intramembranous particles (IMPs) in freeze-fracture replicas like those seen in the rod outer segment (ROS). The proximal zone corresponded in freeze-fracture images to a zone of consecutive horizontal rows of intramembrane particles (ciliary necklaces) and axoneme-membrane cross-linkers. Although protoplasmic face leaflet IMPs similar to those of the distal cilium and outer segment were less abundant in the inner segment and proximal cilium than in the distal cilium and ROS, they were detected in these zones at low frequency. Cytochemistry with concanavalin A and wheatgerm agglutinin revealed the presence of a well developed glycocalyx in the proximal zone. Although opsin binds both lectins, the results suggest heterogeneity among the glycoconjugates of the three membrane domains. Our data define distinct membrane domains of the developing photoreceptor cilium that have important implications for the mechanisms for delivering and sequestering opsin in the outer segment. They also establish that the mechanism of opsin delivery to the distal zone occurs well in advance of the period of disc morphogenesis.

Received May 25, 1984; Revised October 22, 1984;
Accepted October 24, 1984

[1] Our hearty thanks to David Papermaster for a generous supply of antibody and to Win Sale for many useful discussions. This work was supported by National Institutes of Health Research Grant EY03222, Research Career Development Award EY00169 to J. C. B., and Postdoctoral Fellowship EY05646 to D. M. D. Preliminary reports of these results have appeared in abstract form (Besharse and Forestner, 1983; Forestner and Besharse, 1983).

[2] To whom correspondence should be addressed.

Retinal photoreceptors provide a unique opportunity for the study of neuronal polarity related to membrane turnover and the formation of functional membrane domains. The membranous rod outer segment (ROS) consists of photosensitive discs surrounded by a plasma membrane and is connected to the cell body by a non-motile cilium (Röhlich, 1975). The dominant intrinsic protein of the ROS is opsin, the apoprotein of visual pigment (Hall et al., 1969). Whereas opsin is largely restricted to the ROS (Jan and Revel, 1974; Papermaster et al., 1978), an Na^+/K^+ ATPase responsible for generation of the photoreceptor dark current (Hagins, 1972) is restricted to the inner segment (Stirling and Lee, 1980). The zone of demarcation separating these distinctive membrane domains appears to be in the region of the connecting cilium.

Throughout life the ROS turns over by a process involving assembly of new discs from ciliary plasmalemma, their transport distally, and their eventual loss from the ROS distal tip (Young and Bok, 1969; Young, 1976). Opsin and other membrane components are synthesized in the inner segment, transported to the periciliary region, and rapidly consumed in the process of disc assembly (Young, 1967; Young and Droz, 1968; Papermaster et al., 1975). Opsin is a transmembrane glycoprotein (Fukuda et al., 1979; Hargrave, 1982) that is initially synthesized on rough endoplasmic reticulum (RER) (Young and Droz, 1968; Hall et al., 1969). It is co-translationally inserted into RER membrane (Goldman and Blobel, 1981) and then transferred to the Golgi complex for further processing prior to transport to the cilium (Papermaster et al., 1978). Throughout its sojourn in the cell, opsin appears to be associated with membranous organelles. A fundamental question for which only provisional data are available relates to the mechanism of delivery and concentration of opsin in the ROS while maintaining the distinctive properties of inner and outer segment membranes.

Recent morphological, freeze-fracture, immunocytochemical, and autoradiographic data (Holtzman et al., 1977; Kinney and Fisher, 1978; Papermaster et al., 1979, 1985; Besharse and Pfenninger, 1980; Besharse and Forestner, 1981; Defoe and Besharse, 1985) have identified a population of smooth membranous vesicles and cisternae in the periciliary region as the principal organelles of opsin transport to the site of disc assembly. The events occurring in the ciliary region that lead to disc morphogenesis are less well defined. Largely on the basis of freeze-fracture analysis we have suggested that opsin-containing vesicles fuse with the inner segment plasma membrane near the cilium and that membrane components destined for incorporation into discs are transferred to the disc-forming region via the ciliary plasmalemma (Besharse and Pfenninger, 1980). The elaborately developed periciliary ridge complex of frog photoreceptors may play a role in exocytotic fusion and shunting of components into the cilium (Andrews, 1982; Peters et al., 1983). Such a mechanism implies that the ciliary region is capable of concentrating membrane components distally against a concentration gradient and restricting the lateral mobility of those components in order to

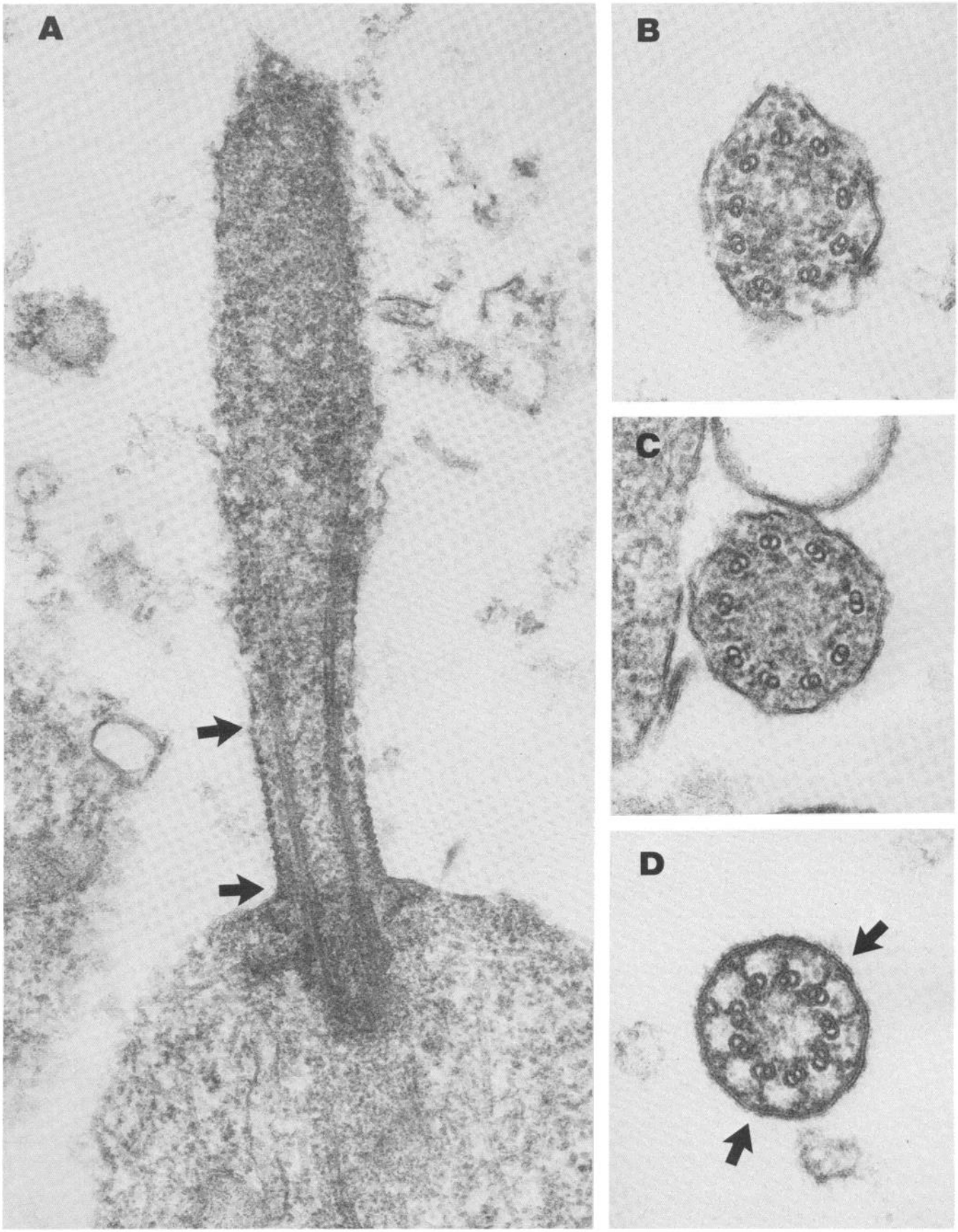
A
B
C
D

maintain the distinctive characteristics of inner and outer segment membranes.

To analyze further the role of the cilium in these processes, we have carried out a morphological analysis of the cilium of neonatal rats using freeze-fracture, immunocytochemistry with anti-opsin, and lectin cytochemistry. We chose neonatal rats for these studies because the entire process of ROS formation occurs postnatally (Weidman and Kuwabara, 1969; Galbavy and Olson, 1979), and because the small size and high density of photoreceptors in their retinas enabled us to observe large numbers of cilia in sections. Our principal results are that the ciliary plasma membrane consists of distinct proximal and distal domains with unique structural properties and that those domains have different binding affinities for anti-opsin and lectins. Even during the period prior to disc formation opsin is concentrated in the distal region from which discs form. The results suggest that the unique proximal zone of the cilium plays a role in transport of opsin to the distal cilium, as well as the maintenance of distinct membrane domains.

Materials and Methods

Animals and fixation of retinas. Fisher strain rats were obtained at 3, 5, 6, 7, 9, 11, and 15 days of postnatal development; three additional experiments were carried out on 3-day-old Sprague-Dawley rats. It is important to point out that we studied photoreceptors at postnatal days 3, 5, 7, and 9 most intensively. At later stages, when ROS had developed, we encountered difficulty in obtaining uniform penetration of reagents into the spaces between photoreceptors. Poor penetration was directly related to the presence of an anionic interphotoreceptor matrix which was difficult to remove by simply washing retinas in a buffer (Defoe et al., 1982; Wood et al., 1984). Animals were sacrificed by cervical dislocation and eyes were removed surgically. After removal of the cornea, iris, and lens, retinas were dissected from eye cups in 0.01 M phosphate buffer containing 0.14 M NaCl at pH 7.2 (PBS). They were then washed in three changes of PBS (30 min) before fixation. In some experiments dissections were carried out in Earles' balanced salt solution (Gibco Laboratories, Grand Island, NY) with or without 0.02% bovine serum albumin (BSA) obtained from Sigma Chemical Co. (St. Louis, MO). This salt solution was gassed with 95% O_2/5% CO_2 to obtain an equilibrium pH of 7.5. Retinas subsequently used for lectin cytochemistry or conventional freeze-fracture were fixed for 1 hr on ice in a mixture containing 2.5% glutaraldehyde, 2% paraformaldehyde and 0.065 M phosphate buffer at pH 7.4. Those used in immunocytochemistry were fixed in 1.25% glutaraldehyde in the same buffer. Fixed retinas were washed in PBS (twice for 10 min) and in PBS containing 1 mM glycine (once for 5 min) to neutralize any available aldehyde groups from glutaraldehyde. For purely structural analysis some preparations were fixed in a mixture of glutaraldehyde-saponin and tannic acid according to the procedure of Maupin and Pollard (1983). This was particularly useful in clarifying structural details of the proximal cilium.

Freeze-fracture. Retinas used for freeze-fracture were gradually infiltrated with 25% glycerol in 0.065 M phosphate buffer and then frozen on gold-nickel specimen supports in Freon 22 cooled with liquid nitrogen. They were stored in liquid nitrogen until fracturing in a Balzers 400T freeze-fracture unit. They were fractured at −116°C under a vacuum of $\leq 1 \times 10^{-6}$ torr and were etched 30 sec before evaporation of platinum from an electron beam gun. Replica thickness (~2.0 nm) was controlled automatically with a quartz crystal thin film monitor. Replicas were backed with about 25 nm of carbon before transfer to 2.0 M NaCl. The NaCl solution was gradually replaced with Chlorox to remove tissue, and after washing, replicas were picked up on Formvar-coated grids for microscopy. For quantitative analysis of intramembrane particle (IMP) density we used a transparent overlay divided into a grid of squares calibrated to represent an area of 0.01 μm^2 on study prints with a final magnification of × 100,000. IMPs were measured (i.e., greatest shadow width perpendicular to shadow direction) to the nearest nanometer on the same prints using a micrometer mounted in a × 7 hand lens.

Immunocytochemistry with Anti-opsin. Retinas were first washed in 0.1 M Tris-HCl (pH 7.4) containing 1% BSA (Tris-BSA) prior to carrying out an indirect localization procedure. All reagents were prepared in Tris-BSA. We used affinity-purified, biotinylated sheep anti-bovine opsin IgG at concentrations of 0.03 to 0.18 mg/ml as the first stage ligand. This antibody has been characterized extensively (Papermaster et al., 1978) and was generously provided by Dr. David S. Papermaster. Purification was carried out with purified bovine opsin coupled to sepharose (Papermaster et al., 1978). It was biotinylated using *N*-hydroxysuccinimide ester, according to the procedure of Heitzman and Richards (1974), and was detected by avidin-ferritin prepared by the method of Heitzman and Richards (1974) or obtained directly from Vector Laboratories (Burlingame, CA).

To examine antibody specificity under conditions similar to those of our immunocytochemistry experiments we separated proteins of a crude preparation of rat outer segments prepared as in the preceding paper (Defoe and Besharse, 1985) or whole retina on 8 to 18% polyacrylamide gradient gels using essentially the method of Laemmli (1970). Immunoreplicas were prepared and stained using the procedures described in the preceding paper (Defoe and Besharse, 1985). The only protein staining specifically in any of the immunoreplicas was opsin (37,000 daltons) and its dimer, trimer, and tetramer. The latter characteristically form in our discontinuous SDS-polyacrylamide system.

Controls for specific binding of anti-opsin in the immunocytochemistry experiments were carried out in each separate labeling experiment. These involved use of biotinylated IgG of the preimmune serum at the same IgG concentrations as those for specific IgG followed by avidin-ferritin, or treatment with avidin-ferritin without prior treatment with antibody. Ferritin grains were rare on tissues treated by either procedure. After labeling with anti-opsin or preimmune serum for 90 min, retinas or retina pieces were washed in Tris-BSA (three times for 20 min) and then incubated 120 min in Tris-BSA containing 0.033 mg/ml of avidin-ferritin. Avidin-ferritin at 0.2 mg/ml was used in one experiment on 3-day-old Sprague-Dawley rats and yielded the same result as that seen with the lower concentration used in most experiments. Retinas were then washed again in 0.15 M NaCl with 1% BSA (three times for 20 min), fixed in 2.5% glutaraldehyde in 0.065 M phosphate buffer, washed in the same buffer containing 0.2 M sucrose, and then postfixed in 1% OsO_4 for 1 hr. Tissues were subsequently dehydrated with ethanol and propylene oxide and embedded in a mixture of Epon 812 (or Embed 812) and Araldite. Thin sections (silver) were analyzed at the Philips 400 electron microscope after staining with bismuth subnitrate (Ainsworth and Karnovsky, 1972) or lead citrate (Reynolds, 1963) and uranyl acetate (Watson, 1958). Bismuth staining enhanced contrast of ferritin grains but provided less contrast of tissue and cell coat.

Cytochemistry with lectins. Lectin binding was analyzed by both direct and indirect procedures. For direct labeling, ferritin conjugates of concanavalin A (Con A) or wheatgerm agglutinin (WGA) were obtained from E-Y Laboratories (San Mateo, CA). Fixed tissue was incubated in PBS containing the conjugate at concentrations from 0.3 to 1.0 mg/ml for periods of 30 to 110 min followed by washing and processing as described above for immunocytochemistry. For localization of unconjugated lectins with colloidal gold, native lectins obtained from E-Y Laboratories were prepared in PBS at concentrations of 0.25 to 1.0 mg/ml. Tissue was incubated for 90 min in lectin solution and were then washed in 0.1 M phosphate buffer at pH 7.4 (three times for 10 min). Colloidal gold (20 nm in diameter) was prepared from chloroauric acid (Polysciences, Warrington, PA) and was coated with horseradish peroxidase (HRP; type II, Sigma) or ovomucoid (Sigma) by the procedures of Geoghegan and Ackerman (1977). HRP-gold and ovomucoid gold, used respectively for detection of Con A and WGA, were suspended in 0.1 M phosphate buffer containing 4% polyvinylpyrrolidone and 0.02% polyethylene glycol (PBP). Lectin-labeled tissues were incubated in the appropriate colloidal gold suspension for 30 min to 12 hr, washed in PBP (three times for 10 min), and then processed for microscopy as described under "Immunocytochemistry with anti-opsin." We have also used biotinylated Con A (Vector Laboratories) at 1 mg/ml which was detected with avidin-ferritin (see above). The procedure was essentially that described under "Immunocytochemistry with anti-opsin" except that solutions were prepared in PBS instead of Tris-BSA.

Controls for specificity of labeling were carried out with each experiment. In direct labeling procedures incubations were carried out in solutions containing 0.1 M α-methylmannopyranoside (Polysciences) or *N,N'*-diacetylchitobiose (Polysciences or Sigma) as hapten sugars for Con A and WGA,

Figure 1. Thin sections of photoreceptor cilia from 7-day-old rats illustrating longitudinal differences in the ciliary membrane. Tissue was fixed by the tannic acid-saponin-glutaraldehyde method (Maupin and Pollard, 1983). Sections were stained with uranyl acetate and lead citrate. *A*, Longitudinal section through the full length of the cilium and part of the inner segment. *Arrows* indicate the region referred to in this paper as the proximal zone. *B* and *C*, Cross-sections from the distal to the middle region of the cilium. *D*, Cross-section in the proximal zone. *Arrows* indicate the region of axoneme-membrane cross-links. Note that detergent disruption of the plasma membrane was more extensive in the distal cilium and inner segment. Magnification, *A*: × 72,250; *B*: × 117,000; *C* and *D*: × 119,000.

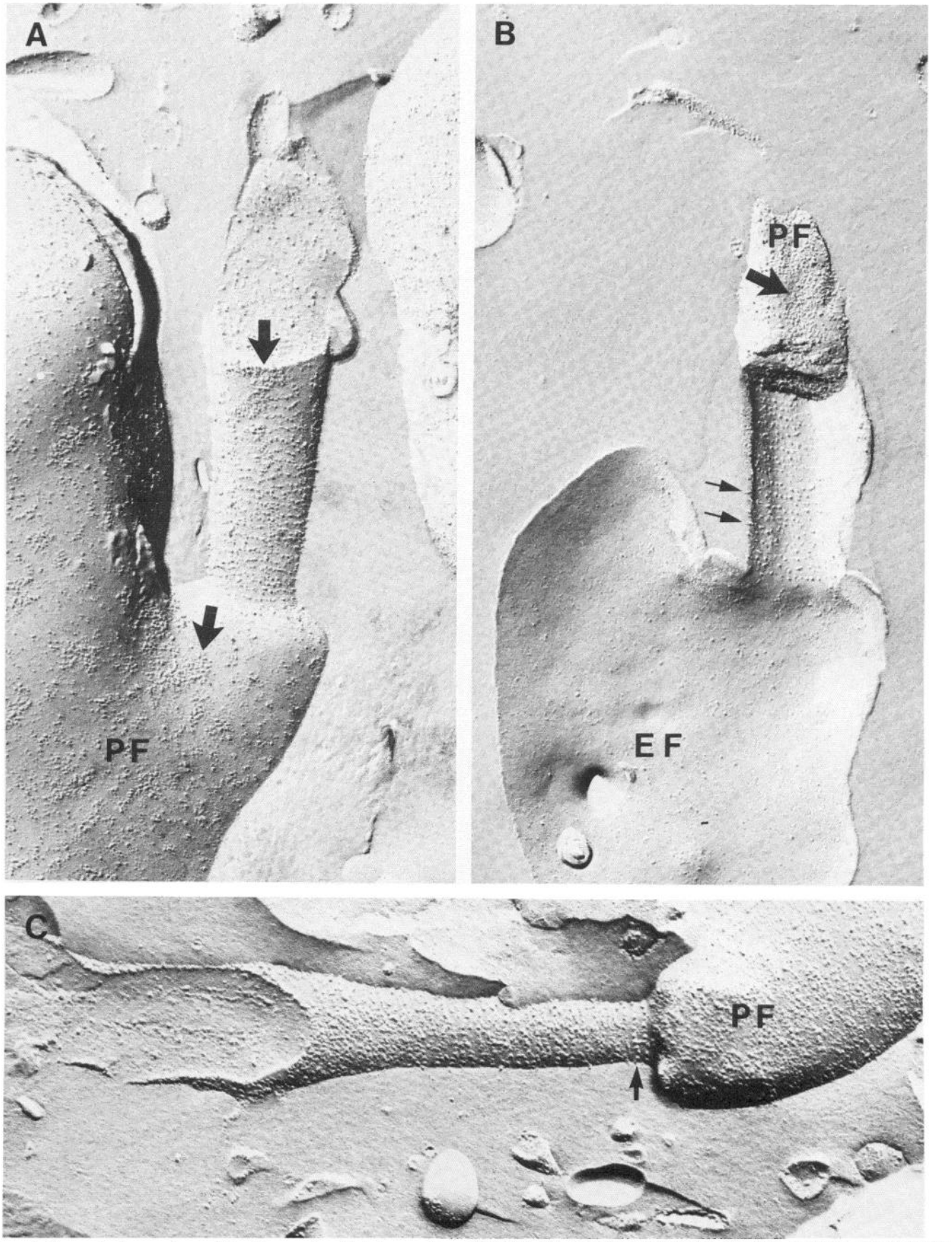

Figure 2. Freeze-fracture replicas of the ciliary region of photoreceptors of 6- (*C*), 7- (*A*), and 9-day-old rats (*B*). *Shadows* are *white* and shadowing direction is from the *bottom*. *Large arrows* indicate IMP clusters and *small arrows* indicate IMP rows of ciliary necklaces. Note that multiple ciliary necklaces as in *B* were readily detected in all replicas of the EF leaflet. Ciliary necklaces were more variable in both distinctness and number on PF leaflets. *EF*, extracellular fracture leaflet; *PF*, protoplasmic fracture leaflet. Magnification × 75,000.

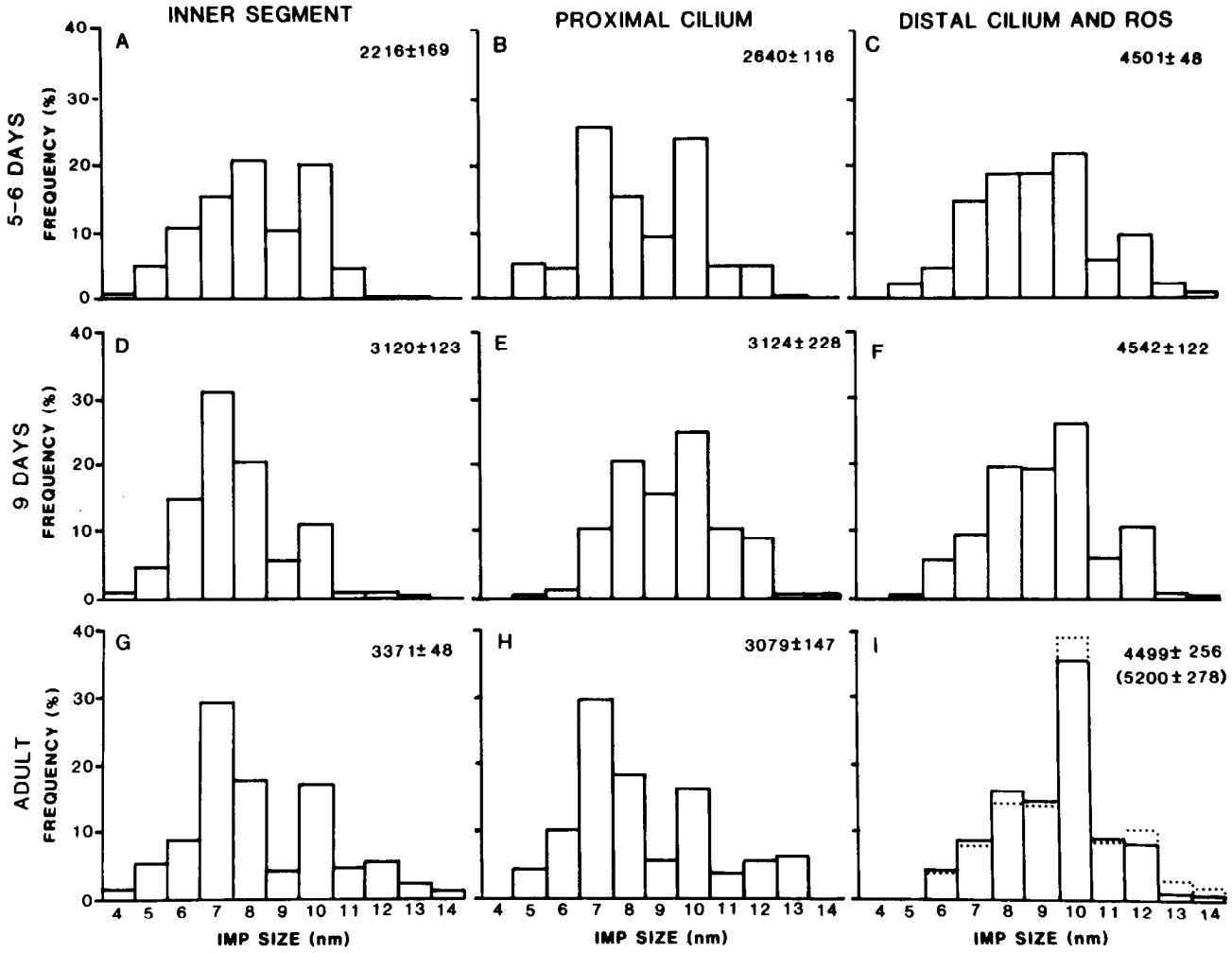

Figure 3. Size frequency distribution of PF leaflet IMPs in three different membrane domains (*top:* inner segment, proximal cilium, and distal cilium-ROS) at three developmental stages (*left:* 5 to 6 days, 9 days, and adult). The density value with each histogram is the average IMP density per square micrometer ± standard error. In *I* the IMP distribution in fractured discs is superimposed (*dotted lines*) over that for outer segment plasma membrane (*solid lines*). IMP in discs is given parenthetically. The higher density in discs is due to the lack of IMP-free patches in disc membranes and their presence in plasma membrane. Data in *C* and *F* are based entirely on distal ciliary membrane or plasma membrane of budding outer segments. Frequency distributions are based on samples as high as 353 IMPs (*D*) to as low as 79 IMPs (*E*) and represent pooled data from many photoreceptors in each domain. The number of measurements in *E* was limited by a lack of fractures through the appropriate region.

respectively. For the indirect procedures the same hapten sugars were used to block binding of the first stage ligand. Both colloidal gold and avidin-ferritin were also used without the first stage ligand to test for nonspecific binding of the detector. The hapten sugars reduced surface labeling to a negligible level, and nonspecific binding of the second stage detectors was virtually absent.

Results

Structure of the developing cilium. Cilia were present on virtually all photoreceptors on the third postnatal day, but disc formation was not seen in any preparation until day 5. As described previously by others (Tokuyasu and Yamada, 1959; Galbavy and Olson, 1979; Greiner et al., 1981), outer segment development initially involved formation of a bulbous expansion of the distal cilium which contained irregular discs. Thin section images of developing photoreceptors even prior to the formation of discs revealed the existence of three distinct membrane domains; inner segment plasma membrane, proximal cilium, and distal cilium. These regions were particularly evident in retinas fixed with the glutaraldehyde-saponin-tannic acid technique which enhanced structural detail in the proximal ciliary region (Fig. 1). The proximal cilium exhibited an array of globular membrane structures (Fig. 1*A*) and axoneme membrane cross-linkers. The latter were most easily detected in cross-section (Fig. 1*D*), where they typically appeared as Y-shaped structures with a broad zone of attachment to the membrane. Saponin in the fixing solution readily disrupted both inner segment (Fig. 1*A*) and distal ciliary (Fig. 1, *B* and *C*) membranes. In the distal cilium, doublet microtubules of the axoneme diverged, axoneme-membrane cross-links were less readily detected, and the membrane bilayer exhibited a greater degree of disruption.

Additional structural distinctions of inner segment, proximal cilium, and distal cilium were revealed in analysis of IMPs of freeze-fracture replicas (Fig. 2). The distal ciliary membrane as early as day 5 contained densely packed IMPs on protoplasmic face (PF) leaflets which were similar in size distribution to those of the outer segment plasma membrane and discs of mature photoreceptors (Fig. 3). The principal developmental change was an increase in the frequency of IMPs of about 10 nm diameter in the adult. The significant decrease in density in adults was due to the existence in adult photoreceptors of expanses of IMP-free areas in the outer segment plasma membrane. These IMP-free areas, described previously as regions enriched in cholesterol (Andrews and Cohen, 1979), represented a significant proportion of outer segment plasma membrane. Their inclusion in the random sampling procedure resulted in an overall decrease in IMP density compared to discs in which IMP-free

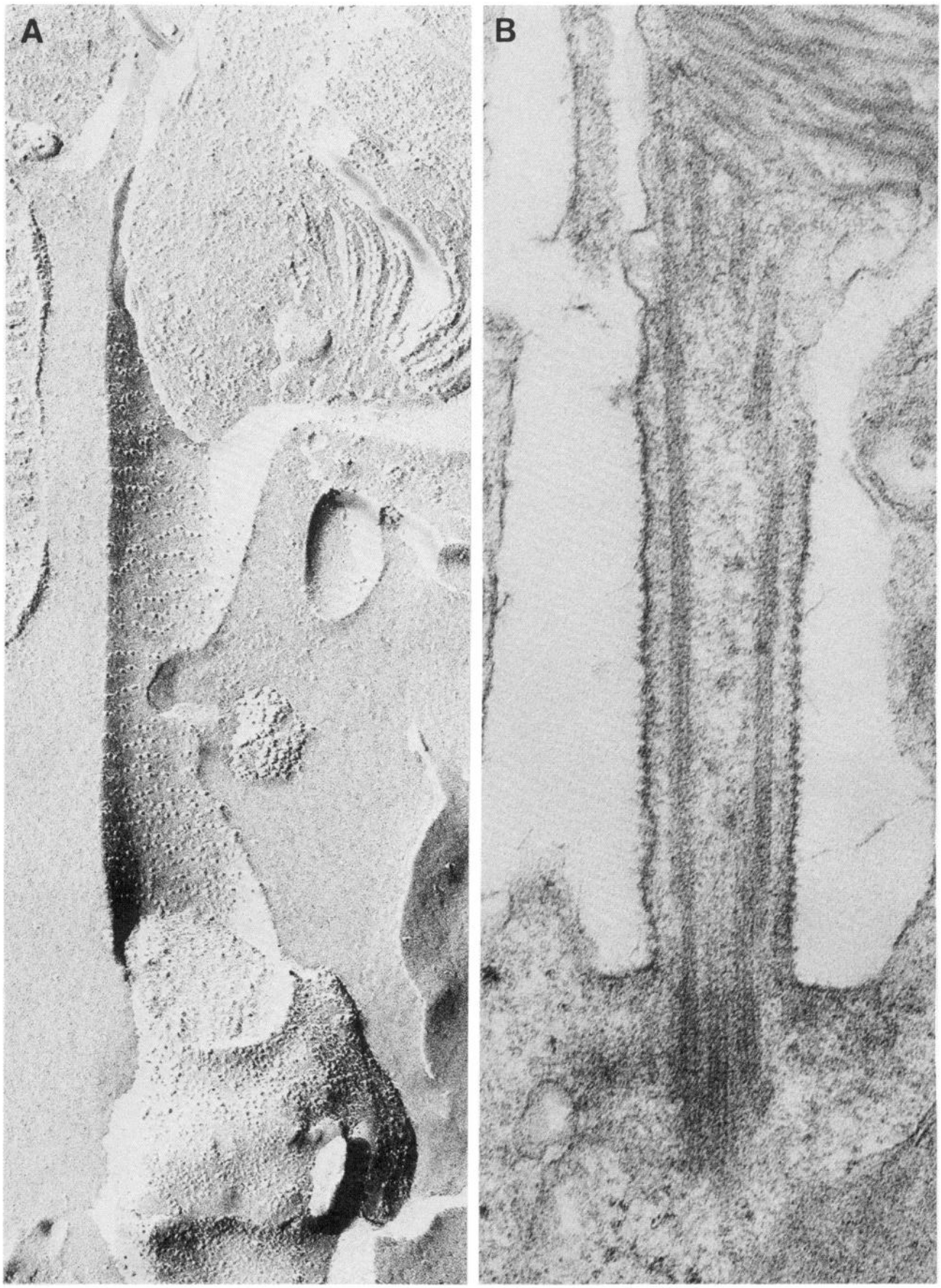

Figure 4

areas were not detected (cf. Fig. 3). Although a broad range of IMP sizes was detected at the early stages of development (Fig. 3, *C* and *F*), discrete classes of IMP sizes such as those reported for developing mouse outer segments (Olive and Recouvreur, 1977) were not detected.

The IMP density and size distributions seen in the distal cilium and outer segment are similar to those reported previously for opsin-containing membranes (see Besharse and Pfenninger, 1980). This IMP pattern differed from that in the proximal cilium and inner segment where a bimodal distribution was routinely seen (Fig. 3). In many preparations, large IMPs similar to those of the outer segment or distal cilium were found largely as aggregates surrounded by dispersed IMPs of smaller size (Fig. 2*A*). This pattern was particularly evident in the inner segment plasma membrane (Fig. 2*A*). In both inner segment and proximal cilium the bimodal distribution of IMP sizes exhibited peaks at 10 and 7 to 8 nm (Fig. 3). The principal developmental change was an increase in inner segment IMP density between days 5 and 9 which involved particles primarily of smaller size (cf. Fig. 3, *A* and *D*). The fluctuations in average IMP density in the proximal cilium (Fig. 3, *B*, *E*, and *H*) may have involved sampling error since relatively fewer fractures revealed this membrane domain, particularly in the sample at 9 days (Fig. 3*E*).

An additional feature of the proximal cilium was a tendency for IMPs of PF leaflets to be arranged in rows perpendicular to the ciliary long axis (Fig. 2, *A* and *C*). IMPs of the rows were generally of the smaller size, whereas those of large size often occurred as larger aggregates similar to those aggregates seen in the inner segment (Fig. 2*A*). The IMP rows were not always distinct; in some cells short linear arrays of IMPs were seen and IMP density increased in a proximal to distal gradient (Fig. 2*C*). This kind of trend in the arrangement of IMPs in PF leaflets was not related to developmental age. Similar variability was detected at each stage examined, including adults.

In contrast to the somewhat variable arrangement of IMPs on PF leaflets of the proximal cilium, those of the exoplasmic face (EF) leaflet were invariably arranged in the form of horizontal rows which contrasted dramatically with IMPs of the EF leaflets of adjacent inner segment plasma membrane (Figs. 2*B* and 4*A*). The average density of these IMPs (1700 to 2200/μm^2; area includes space between rows) was substantially greater than the average of EF leaflet densities of 499 and 332/μm^2, respectively, for inner segment and distal ciliary membranes. Their size distribution in different preparations was unimodal with a peak representing 30 to 40% of the IMPs at 7 to 8 nm. The rings of IMPs on EF leaflets had an average repeat period of about 32 nm. This period corresponded closely to that of surface densities seen in thin sections (Fig. 4*B*). After the ROS had formed (i.e., after day 5), the EF leaflet rings were found throughout the length of the connecting cilium proper as described previously for mature rat cilia (see Fig. 4*A*).

Proximal and distal ciliary zones were also distinguishable in cross-sections. In the proximal zone, the plasma membrane formed a near-circular profile around the axoneme and was linked to the axoneme by cross-linkers emanating from the junction of A and B subfibers of each doublet microtubule (Fig. 1*D*). The doublet microtubules appeared to lack distinct dynein arms but in the proximal region were radially associated by intermicrotubule cross-links which formed a dense central ring. The distal region was characterized by an irregular plasma membrane, a lack of plasma membrane-axoneme linkers, and substantial disorder in the arrangement of the axoneme (Figs. 1, *B* and *C*, 5*C*, and 7*D*). It has been suggested that IMPs of EF leaflet rings, axonemal cross-linkers, and surface densities form a complex that may be involved in opsin transport in mature cells (Röhlich, 1975).

Distribution of anti-opsin-binding sites. Anti-opsin-binding sites were found in high density on the plasma membrane of the distal cilium at all developmental stages examined (Figs. 5 and 6). In cells with formed ROS, anti-opsin binding was primarily associated with the ROS plasmalemma where it was densely and uniformly distributed (Fig. 6*A*). Binding also extended onto the distal ciliary region from which discs form (Fig. 6*A*). Binding sites were also evident at focal sites on the inner segment plasma membrane, but overall binding in the latter region was low compared to that of the ROS or distal cilium (Fig. 6*A*). In the proximal ciliary zone, binding density was also low; in many cells anti-opsin binding was entirely lacking in this region (Figs. 5, *A*, *B*, *D*, and *E*, and 6*A*).

At postnatal days, 5, 7, and 9 this pattern of anti-opsin labeling was applicable to virtually all cells examined. At postnatal day 3, a period prior to initial disc formation, labeled cells all exhibited the distinct pattern illustrated in Figure 5. However, since all cells examined were not labeled, we carried out a frequency analysis of labeling patterns seen in the central retina which included a total of 532 photoreceptors. In 17 cells in which the entire ciliary shaft was visible, 9 exhibited the differentiated labeling pattern seen in Figure 5*D*. The other 8 cells had no label at all. Cell bodies were identified in all cells analyzed. Nine percent (48 cells) exhibited inner segment labeling that was of substantially higher density than described above. The remaining 91% exhibited either no label or occasional focal patches of label like that seen at later stages of development.

Distribution of glycoconjugates. Opsin is a glycoprotein that binds both Con A and WGA (Molday and Molday, 1979; Steinemann and Stryer, 1973). Therefore, we evaluated the distribution of Con A- and WGA-binding sites for comparison to the distribution of opsin. Each ligand exhibited a general distribution over all photoreceptor surfaces. Con A-binding sites were associated with the plasma membrane, ciliary cell coat, and interphotoreceptor matrix (Fig. 7). All were specific as determined by hapten sugar inhibition (Figs. 4*B* and 8*A*). The labeling density throughout the cilium was consistently higher than that of the inner segment plasma membrane. The binding of Con A to the proximal cilium was largely associated with the thick cell coat of this region (Figs. 7 and 8*C*). In this region ferritin or gold particles were seen at variable distances from the membrane proper (Fig. 8*C*). In the distal cilium and developing ROS, however, binding sites were more closely associated with the membrane surface (Figs. 7 and 8*B*). Biotinylated Con A detected by avidin-ferritin using procedures similar to those in the immunocytochemistry revealed the same overall pattern of Con A binding.

Both indirect and direct labeling procedures revealed a similar pattern of WGA-binding sites on developing cells. WGA followed by ovomucoid-gold resulted in abundant labeling of the ciliary proximal zone (Fig. 9). In most preparations fewer binding sites were detected in the distal ciliary zone and inner segment plasma membrane. Cross-sectional profiles exhibited dense packing of colloidal gold. However, occasional tangential sections suggested that WGA-binding sites were arranged in horizontal arrays reminiscent of those of IMPs seen on PF leaflets of the fractured proximal zone (Fig. 9*E*). Abundant binding sites were also detected in the space surrounding cells: the interphotoreceptor matrix. This binding increased dramatically as outer segments developed and was so enriched with WGA-binding sites that penetration of ligand was reduced at later developmental stages and in adults.

Discussion

Structure of the developing photoreceptor cilium. Although morphogenesis of photoreceptor cilia has been described in several mammalian species (Tokuyasu and Yamada, 1959; DeRobertis, 1960; Galbavy and Olson, 1979; Greiner et al., 1981), their structure

Figure 4. Freeze-fracture view of ciliary necklace IMP rows on an EF leaflet of the cilium of an adult (*A*) and thin section view of an 11-day rat photoreceptor cilium (*B*). Note that *B* was incubated with 0.1 M α-methylmannopyranoside and Con A as a control for specificity of Con A binding (see Figs. 7 and 8). This figure illustrates the cell coat material associated with the proximal cilium. Note that the repeat period of both IMP rows and surface globules is about 32 nm. Magnifications, *A:* × 93,000; *B:* × 94,500.

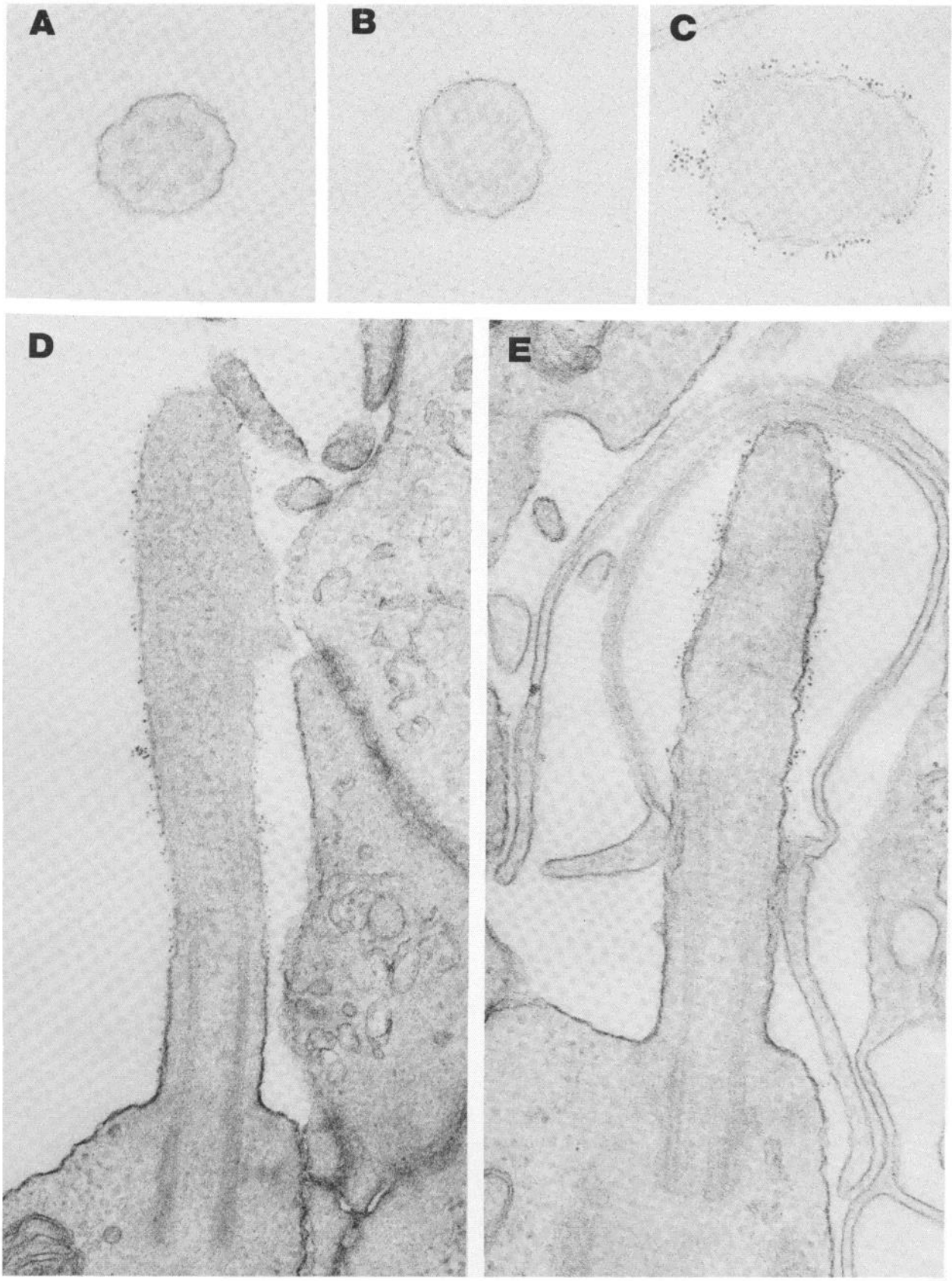

Figure 5. Localization of opsin in the distal zone of photoreceptor cilia of 3-day-old rats. All cells were stained with bismuth subnitrate. *A* and *B* are cross-sections through the proximal cilium and *C* is through the distal cilium. *D* and *E* are longitudinal sections. In *E*, processes from an adjacent pigment epithelial cell, identifiable in a larger field of view, surround the cilium. Individual retinal pigment epithelial cells occasionally remain adherent to retinas during isolation. As seen here, the presence of an adjacent retinal pigment epithelium cell did not prevent penetration of anti-opsin to the cilium, nor were membranes other than that of the distal cilium significantly labeled. Although focal labeling of inner segment plasma membranes is often seen, it is not apparent in *D* or *E*. Magnifications, *A* to *C:* × 104,500; *D:* × 68,750; *E:* × 84,250.

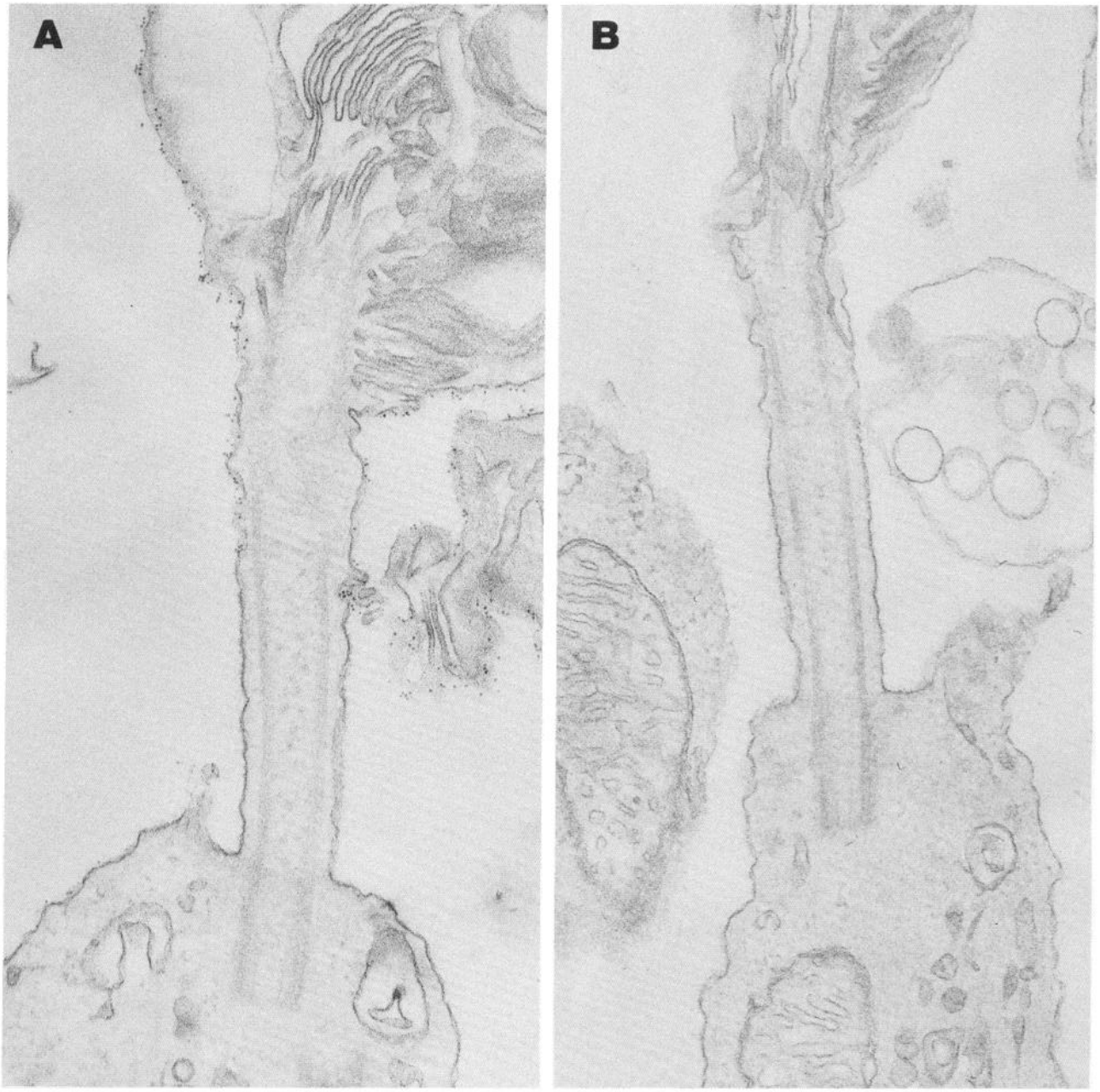

Figure 6. Anti-opsin labeling of photoreceptors of 11-day-old rats. *A*, Outer segment and distal ciliary labeling. A few ferritin grains are also seen on the inner segment plasma membrane. *B*, Control cell from a preparation treated identically to *A* except that preimmune IgG replaced anti-opsin IgG. Magnification × 63,750.

remains poorly defined. A basic finding in our study is that photoreceptor cilia from the earliest developmental stage examined have properties in common with those described previously for adult rat (Matsusaka, 1974; Röhlich, 1975). Thus, prior to initial disc formation we have described two structural zones: a proximal zone which corresponds to what has been called the transitional zone of both adult photoreceptors (Röhlich, 1975) and motile cilia (Gilula and Satir, 1972) and a distal zone which corresponds to the outer segment and disc-forming region of mature photoreceptors (Röhlich, 1975). The principal structural features of the proximal zone include a dense surface coat, "bead-like" membrane structures with a longitudinal repeat period of about 32 nm, horizontal rows of IMPs (ciliary necklaces) on EF leaflets with an average repeat period of about 32 nm, and more densely packed IMPs in the PF leaflet, generally arranged as linear arrays or rows. Cross-linkers between doublet microtubules of the axoneme and the plasma membrane are also evident, particularly in cross-sectional views. Both dynein arms and a central pair of microtubules appear to be lacking (see Matsusaka, 1976). Röhlich (1975) suggested that IMPs of ciliary necklaces and membrane globules are components of a transmembrane complex cross-linked to the axoneme. Although a possible barrier role of such an arrangement is evident, recent evidence from motile cilia suggesting that a membrane-associated ATPase is cross-linked to the axoneme (Dentler et al., 1980) raises the possibility that these structures may also be involved directly in the generation of a highly polarized distribution of opsin.

Distribution of opsin, glycoconjugates, and IMPs. The distribution of immunoreactive opsin, glycoconjugates, and IMPs is best understood in relationship to the structural features outlined above. Opsin was detected in greatest concentration in the distal ciliary zone in early stages and in the ROS plasma membrane at later stages. It was also found at focal sites on the inner segment plasma membrane

Figure 7. Con A labeling by the direct procedure shows heavy labeling over the cilium and developing ROS of a 7-day rat photoreceptor. Label is heaviest over the cilium proper and less dense over the inner segment plasma membrane. Note the association of Con A with the cell coat some distance from the plasma membrane in the proximal ciliary region. Magnification × 57,500.

but was rarely detected in the ciliary proximal zone. This distribution for developing photoreceptors is comparable to that reported for mature rat (Papermaster and Schneider, 1982; Nir et al., 1984) and frog (Nir and Papermaster, 1983) photoreceptors. The differentiated labeling pattern is also comparable to that recently reported for developing rat photoreceptors at postnatal day 5 and later (Nir et al., 1984). Although the latter authors emphasized labeling of the inner segment plasma membrane prior to postnatal day 21, they also demonstrated a paucity of label in the proximal cilium and concentration of label in the distal cilium. Our observations differ principally in that we detected substantially less labeling of the inner segment plasma membrane at all stages examined, and we obtained positive evidence for preferential accumulation of opsin in the distal cilium during postnatal day 3. The latter observation is of some importance because it shows that, prior to the onset of disc morphogenesis, a mechanism exists for delivery and concentration of opsin in distal ciliary membrane.

The pattern of anti-opsin labeling was not congruent with the distribution of glycoconjugates detected by Con A and WGA. Even though opsin binds both lectins (Steinemann and Stryer, 1973; Molday and Molday, 1979), we found that the proximal cilium, the region of lowest opsin density, bound both lectins to its cell coat, and the reaction with WGA in this zone was generally more intense than in distal cilium or inner segment. This observation suggests a degree of heterogeneity in the nature of the glycoconjugates in the three membrane domains. The well developed cell coat in the zone of lowest opsin immunoreactivity also raises the possibility that some antigenic determinants are "masked" by cell coat material. However, the generalized distribution of lectin-binding sites over inner segment plasma membrane, proximal cilium, and distal cilium using several different detection systems suggests that the differentiated pattern of anti-opsin-binding sites cannot be explained trivially as lack of access of reagents to all cell surfaces.

The extensive labeling of the distal cilium and outer segment plasmalemma with anti-opsin was correlated with a dense array of IMPs in freeze-fracture replicas with a modal size of about 10 nm. Such IMPs have been found to be characteristic of opsin-containing membranes in a variety of species (Hong and Hubbell, 1972; Corless et al., 1976; Besharse and Pfenninger, 1980). In our previous freeze-fracture analysis of mature *Xenopus* photoreceptors (Besharse and

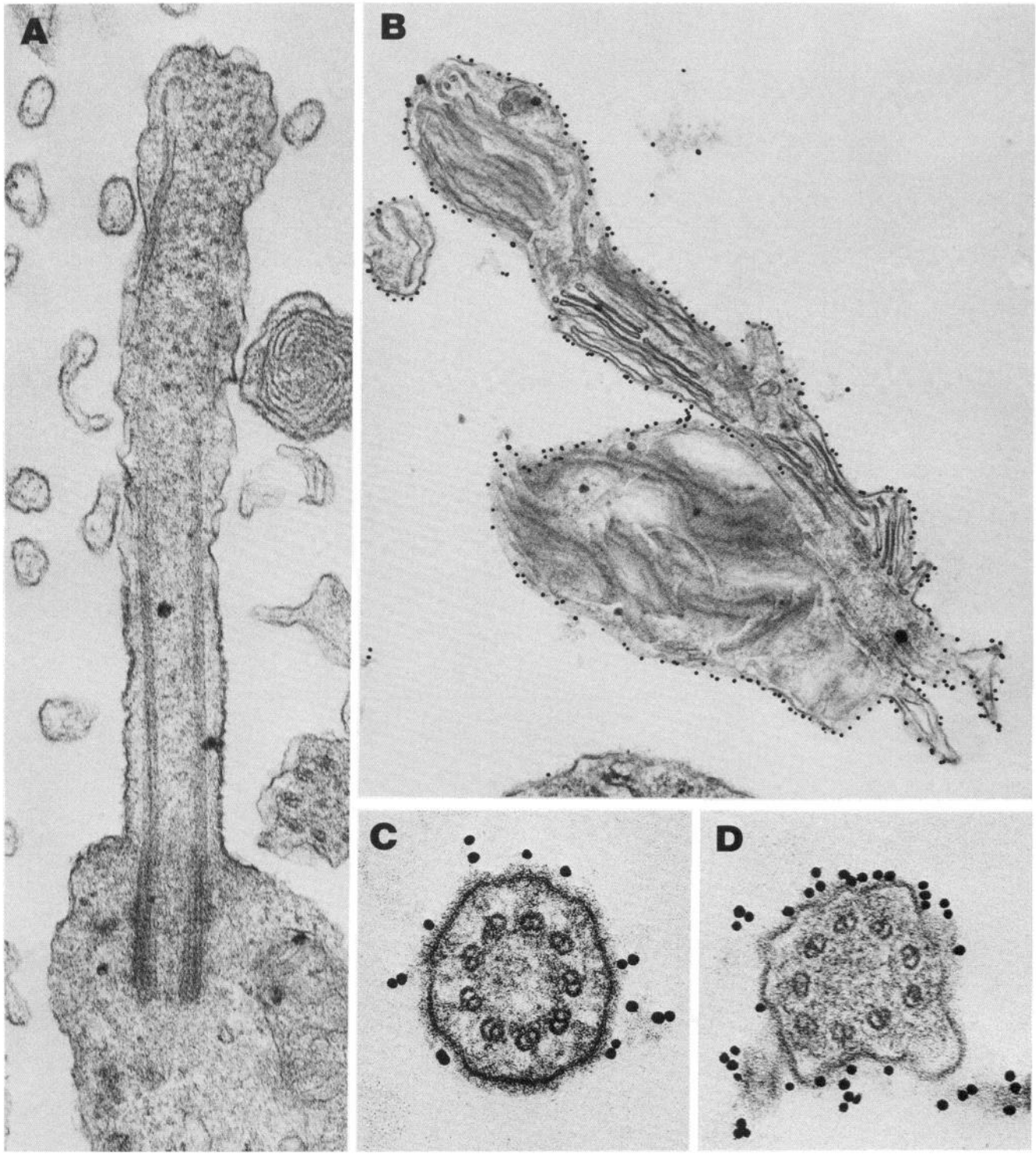

Figure 8. Con A binding revealed by colloidal gold in 5-day rats. *A*, Cell from an incubation treated with 0.1 M α-methylmannopyranoside during the Con A binding step. *B*, Con A binding to the plasma membrane of a developing outer segment. Cross-sections of proximal (*C*) and distal (*D*) cilium are also illustrated. Note the association of Con A with the cell coat some distance from the plasma membrane at the proximal cilium (*C*) and its closer association with the membrane of the outer segment (*B*). Magnifications, *A:* × 82,500; *B:* × 50,750; *C* and *D:* × 113,000.

Pfenninger, 1980), we argued that the similarity in size distribution of IMPs in PF leaflets of ciliary plasma membrane and outer segment suggested identity of a major intrinsic membrane protein of both membrane systems. Because the IMP of PF leaflets in the ROS depends on the presence of opsin (Hong and Hubbell, 1972; Corless et al., 1976), it seemed reasonable to suggest that ciliary and cytomembrane IMPs of similar size also reflected the distribution of opsin. This view is in accord with the present results regarding the distal cilium. Furthermore, the sparse anti-opsin labeling of proximal cilium and inner segment plasma membrane correlates with the relative rarity of larger IMPs in those membrane compartments. IMP distributions in both proximal cilium and inner segment were generally bimodal, and the larger IMPs often formed small aggregates in both zones that were similar in IMP size and packing to those seen in the distal cilium and outer segment. Thus, we find a general correspondence between anti-opsin labeling density and density of

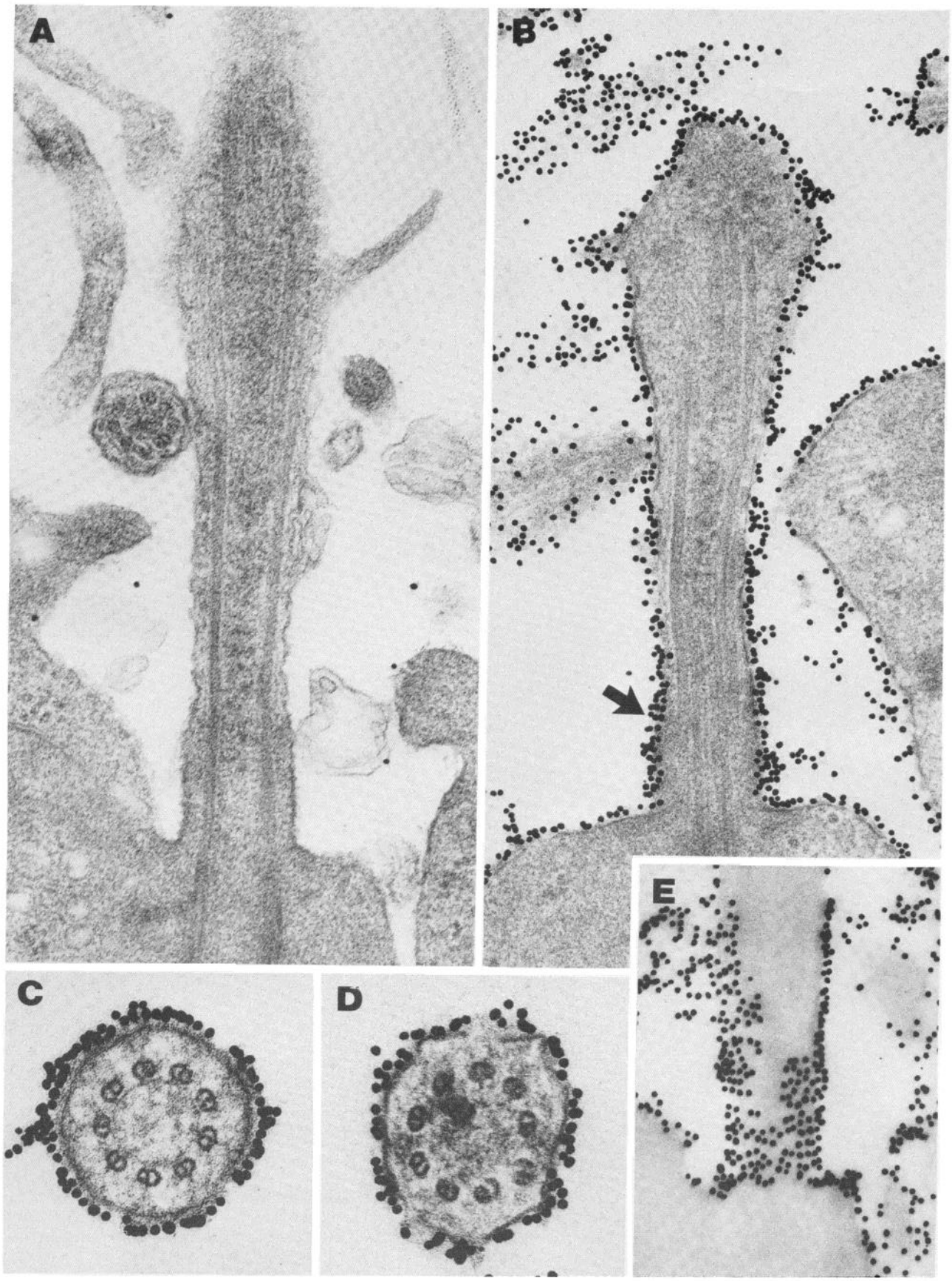

Figure 9. WGA labeling of developing cilium. *A*, A cell from a retina treated with 0.1 M *N,N*-diacetylchitobiose during the lectin-labeling period. *B*, A cell labeled with WGA typically shows heavy labeling over the entire cilium and inner segment plasma membrane. Labeling is heaviest in the proximal cilium (*arrow*). *C* and *D*, Ciliary cross-sections through the proximal and distal zones, respectively. *E*, A longitudinal tangential section of an unstained proximal zone showing the tendency of colloidal gold particles to form scalloped rows reminiscent of ciliary necklaces. *A* to *D*, from 7-day rats; *E*, from 3-day rat. Magnifications, *A:* × 71,750; *B:* × 71,750; *C* and *D:* × 113,500; *E:* × 76,000.

large (10 nm) IMPs in the three membrane domains that is consistent with a model for opsin delivery to the developing cilium from the inner segment plasma membrane (see Besharse and Pfenninger, 1980). It is of some interest that structures comparable to the elaborate periciliary ridge complex of frog photoreceptors (Peters et al., 1983) are not found in either mature or developing rat photoreceptors.

Significance of the proximal ciliary zone. The high concentration of opsin in the distal cilium well in advance of disc morphogenesis allows us to distinguish two fundamentally distinct processes: opsin transport and disc formation. The latter process apparently uses distal ciliary membrane to form evaginations which in rod photoreceptors become separated to form discs (Steinberg et al., 1980). The former process involves the concentration of opsin in the membrane from which discs form. The first stage of opsin transport appears to involve delivery of vesicles to the periciliary region (Papermaster et al., 1979, 1985; Besharse and Pfenninger, 1980; Defoe and Besharse, 1985). From this point, opsin is delivered against a concentration gradient to the distal cilium. Although transfer via the proximal ciliary plasmalemma has frequently been suggested, it should be emphasized that there is no direct evidence for such transfer and that other mechanisms such as vesicular budding from inner segment followed by vesicular fusion with distal cilium are compatible with the results of this study.

Previous observations on the rate of ROS formation and opsin density indicate that, in rats, about 4×10^3 opsin molecules must be delivered to the distal zone per minute. In addition to playing a direct role in directed transport of opsin and other membrane components, the proximal zone may also play a barrier role. Opsin in discs (Poo and Cone, 1973; Liebman and Entine, 1974), and possibly plasma membrane as well, is freely mobile by lateral diffusion, yet is found in exceedingly low concentration in the inner segment plasma membrane. Likewise, the Na^+/K^+ ATPase, a major intrinsic protein of the inner segment, is largely restricted to that location (Stirling and Lee, 1980). Although the mechanisms of ciliary transport and the barrier can only be guessed at presently, our attention must be directed to the highly ordered complex of surface globules, IMPs, and axoneme-membrane cross-links of the proximal region. Structures with the same general organization are found in the motile cilia from protozoa to mammals (Dentler, 1981; Gilula and Satir, 1972) and may play a role in directed membrane motility (Bloodgood, 1977), the genesis of distal ciliary membrane (Satir et al., 1976), and perhaps the maintenance of membrane domains. In sensory cilia of photoreceptors, a primary role for these structures may be in the generation and maintenance of the unique features of the distal ciliary zone and outer segment.

References

Ainsworth, S. K., and M. J. Karnovsky (1972) An ultrastructural staining method for enhancing the size and electron opacity of ferritin in thin sections. J. Histochem. Cytochem. *20:* 225–229.

Andrews, L. D. (1982) Freeze-fracture studies of vertebrate photoreceptor. In *The Structure of the Eye*, J. G. Hollyfield, ed., pp. 11–23, Elsevier-North Holland Publishing Co., New York.

Andrews, L. D., and A. I. Cohen (1979) Freeze-fracture evidence for the presence of cholesterol in particle-free patches of basal disks and the plasma membrane of retinal rod outer segments of mice and frogs. J. Cell Biol. *81:* 215–228.

Besharse, J. C., and D. M. Forestner (1981) Horseradish peroxidase uptake by rod photoreceptor inner segments accompanies outer segment disc assembly. Proceeding of 39th Annual Meeting of the Electron Microscopy Society of America. Claitor's Publishing Division, Baton Rouge, Louisiana.

Besharse, J. C., and D. M. Forestner (1983) Membrane domains of developing photoreceptor cilia revealed by lectins and antiopsin. J. Cell Biol. *97:* 411a.

Besharse, J. C., and K. H. Pfenninger (1980) Membrane assembly in retinal photoreceptors. I. Freeze-fracture analysis of cytoplasmic vesicles in relationship to disc assembly. J. Cell Biol. *87:* 451–463.

Bloodgood, R. A. (1977) Motility occurring in association with the surface of the *Chlamydomonas* flagellum. J. Cell Biol. *75:* 983–989.

Corless, J. M., W. H. Cobbs, III, M. J. Costello, and J. D. Robertson (1976) On the asymmetry of frog retinal rod outer segment disc membranes. Exp. Eye Res. *23:* 295–324.

Defoe, D. M., and J. C. Besharse (1985) Membrane assembly in retinal photoreceptors. II. Immunocytochemical analysis of freeze-fractured rod photoreceptor membrane using anti-opsin antibodies. J. Neurosci. *5:* 1023–1034.

Defoe, D. M., D. M. Forestner, and J. C. Besharse (1982) Photoreceptor anionic binding sites: Contribution of the inter-photoreceptor matrix. Invest. Ophthalmol. Vis. Sci. Suppl. *22:* 142.

Dentler, W. L. (1981) Microtubule-membrane interactions in cilia and flagella. Int. Rev. Cytol. *72:* 1–47.

Dentler, W. L., M. M. Pratt, and R. E. Stephens (1980) Microtubule-membrane interactions in cilia. II. Photochemical cross-linking of bridge structures and the identification of a membrane associated dynein-like ATPase. J. Cell Biol. *84:* 381–403.

DeRobertis, E. (1960) Some observations on the ultrastructure and morphogenesis of photoreceptors. J. Gen. Physiol. *43 (Suppl.2):* 1–13.

Forestner, D. M., and J. C. Besharse (1983) Membrane assembly in photoreceptors: Spatially differentiated labeling of developing photoreceptor cilia with antiopsin and lectins. Invest. Ophthalmol. Vis. Sci. Suppl. *24:* 287.

Fukuda, M. N., D. S. Papermaster, and P. A. Hargrave (1979) Rhodopsin carbohydrate. Structure of small oligosaccharides attached at two sites near the NH_2 terminus. J. Biol. Chem. *254:* 8201–8207.

Galbavy, E. S. J., and M. D. Olson (1979) Morphogenesis of rod cells in the retina of the albino rat: A scanning electron microscopic study. Anat. Rec. *195:* 707–718.

Gilula, N. B., and P. Satir (1972) The ciliary necklace: A ciliary membrane specialization. J. Cell Biol. *53:* 494–509.

Geoghegan, W. D., and G. A. Ackerman (1977) Adsorption of horseradish peroxidase, ovomucoid and antimmunoglobulin to colloidal gold for the indirect detection of Concanavalin A, wheat germ agglutinin and goat anti-human immunoglobulin G on cell surfaces at the electron microscope level: A new method, theory and application. J. Histochem. Cytochem. *25:* 1187–1200.

Goldman, B. M., and G. Blobel (1981) *In vitro* biosynthesis, core glycosylation, and membrane integration of opsin. J. Cell Biol. *90:* 236–242.

Greiner, J. V., T. A. Weidman, H. D. Bodley, and C. A. M. Greiner (1981) Ciliogenesis in photoreceptor cells of the retina. Exp. Eye Res. *33:* 433–446.

Hagins, W. A. (1972) The visual process: Excitatory mechanisms in the primary photoreceptor cells. Annu. Rev. Biophys. Bioeng. *1:* 131–158.

Hall, M. O., D. Bok, and A. D. E. Bacharach (1969) Biosynthesis and assembly of the rod outer segment membrane system. Formation and fate of Visual Pigment in the frog retina. J. Mol. Biol. *45:* 397–406.

Hargrave, P. A. (1982) Rhodopsin chemistry, structure and topography. Prog. Retinal Res. *1:* 1–51.

Heitzmann, H., and F. M. Richards (1974) Use of the avidin-biotin complex for specific staining of biological membranes in electron microscopy. Proc. Natl. Acad. Sci. U. S. A. *71:* 3537–3541.

Holtzman, E., S. Schacher, J. Evans, and S. Teichberg (1977) Origin and fate of the membranes of secretion granules and synaptic vesicles: Membrane circulation in neurons, gland cells and retinal photoreceptors. In *The Synthesis, Assembly and Turnover Cell Surface Components*, G. Poste and G. L. Nicolson, eds., pp. 165–246, Elsevier/North Holland Biomedical Press, New York.

Hong, K., and W. L. Hubbell (1972) Preparation and properties of phospholipid bilayers containing rhodopsin. Proc. Natl. Acad. Sci. U. S. A. *69:* 2617–2621.

Jan, L. Y., and J. -P. Revel (1974) Ultrastructural localization of rhodopsin in the vertebrate retina. J. Cell Biol. *62:* 257–273.

Kinney, M. S., and S. K. Fisher (1978) The photoreceptors and pigment epithelium of the larval *Xenopus* retina: Morphogenesis and outer segment renewal. Proc. R. Soc. Lond. (Biol.) *201:* 149–167.

Laemmli, U. K. (1970) Cleavage of structural proteins during the assembly of the head of bacteriophage T4. Nature (Lond.) *227:* 680–685.

Liebman, P. A., and G. Entine (1974) Lateral diffusion of visual pigment in photoreceptor disk membranes. Science *185:* 457–459.

Matsusaka, T. (1974) Membrane particles of the connecting cilium. J. Ultrastruct. Res. *48:* 305–312.

Matsusaka, T. (1976) Cytoplasmic fibrils of the connecting cilium. J. Ultrastruct. Res. *54:* 318–324.

Maupin, P., and T. D. Pollard (1983) Improved preservation and staining of Hela cell actin filaments, clathrin coated membranes, and other cytoplas-

mic structures by tannic acid-glutaraldehyde-saponin fixation. J. Cell Biol. *80:* 69–76.

Molday, R. S., and L. L. Molday (1979) Identification and characterization of multiple forms of rhodopsin and minor proteins of frog and bovine rod outer segment disc membranes. J. Biol. Chem. *254:* 4653–4660.

Nir, I., and D. S. Papermaster (1983) Differential distribution of opsin in the plasma membrane of frog photoreceptors: An immunocytochemical study. Invest. Ophthalmol. Vis. Sci. *24:* 868–878.

Nir, I., D. Cohen, and D. S. Papermaster (1984) Immunocytochemical localization of opsin in the cell membrane of developing rat retinal photoreceptors. J. Cell Biol. *98:* 1788–1795.

Olive, J., and M. Recouvreur (1977) Differentiation of retinal disc membranes in mice. Exp. Eye Res. *25:* 63–74.

Papermaster, D. S., and B. G. Schneider (1982) Biosynthesis and morphogenesis of outer segment membranes in vertebrate photoreceptor cells. In *Cell Biology of the Eye*, D. S. McDevitt, ed., pp. 475–531, Academic Press, Inc., New York.

Papermaster, D. S., C. A. Converse, and J. Siu (1975) Membrane biosynthesis in the frog retina: Opsin transport in the photoreceptor cell. Biochemistry *14:* 1343–1352.

Papermaster, D. S., B. G. Schneider, M. A. Zorn, and J. P. Kraehenbuhl (1978) Immunocytochemical localization of opsin in outer segments and Golgi zones of frog photoreceptor cells. J. Cell Biol. *77:* 196–210.

Papermaster, D. S., B. G. Schneider, and J. C. Besharse (1979) Assembly of rod photoreceptor membranes. Immunocytochemical and autoradiographic localization of opsin in smooth vesicles of the inner segment. J. Cell Biol. *83:* 275a.

Papermaster, D. S., B. G. Schneider, and J. C. Besharse (1985) Vesicular transport of newly synthesized opsin from the Golgi apparatus toward the rod outer segment: Immumocytochemical and autoradiographic evidence. Invest. Ophthalmol. Vis. Sci., in press.

Peters, K. -R., G. E. Palade, B. G. Schneider, and D. S. Papermaster (1983) Fine structure of a periciliary ridge complex of frog retinal rod cells revealed by ultrahigh resolution scanning electron microscopy. J. Cell Biol. *96:* 265–276.

Poo, M. -M., and R. A. Cone (1973) Lateral diffusion of rhodopsin in *Necturus* rods. Exp. Eye Res. *17:* 503–510.

Reynolds, E. S. (1963) The use of lead citrate at high pH as an electron opaque stain in electron microscopy. J. Cell Biol. *17:* 208–213.

Röhlich, P. (1975) The sensory cilium of retinal rods is analogous to the transitional zone of motile cilia. Cell Tissue Res. *161:* 421–430.

Satir, B., W. S. Sale, and P. Satir (1976) Membrane renewal after dibucaine deciliation of *Tetrahymena*. Exp. Cell Res. *97:* 83–91.

Steinberg, R. H., S. K. Fisher, and D. H. Anderson (1980) Disc morphogenesis in vertebrate photoreceptors. J. Comp. Neurol. *190:* 501–518.

Steinemann, A., and L. Stryer (1973) Accessibility of the carbohydrate moiety of rhodopsin. Biochemistry *12:* 1499–1502.

Stirling, C. E., and A. Lee (1980) [^{3}H]Ouabain autoradiography of frog retina. J. Cell Biol. *85:* 313–324.

Tokuyasu, K., and E. Yamada (1959) The fine structure of the retina studied with the electron microscope. IV. Morphogenesis of outer segments of retinal rods. J. Biophys. Biochem. Cytol. *6:* 225–230.

Watson, M. L. (1958) Staining of tissue sections for electron microscopy with heavy metals. J. Biophys. Biochem. Cytol. *4:* 475–481.

Weidman, T. A., and T. Kuwabara (1969) Development of the rat retina. Invest. Ophthalmol. *8:* 60–69.

Wood, J. G., J. C. Besharse, and L. Napier-Marshall (1984) Partial characterization of lectin binding sites of retinal photoreceptor outer segments and interphotoreceptor matrix. J. Comp. Neurol. *288:* 299–307.

Young, R. W. (1967) The renewal of photoreceptor cell outer segments. J. Cell Biol. *33:* 61–73.

Young, R. W. (1976) Visual cells and the concept of renewal. Invest. Ophthalmol. *15:* 700–725.

Young, R. W., and D. Bok (1969) Participation of the retinal pigment epithelium in the rod outer segment renewal process. J. Cell Biol. *42:* 392–403.

Young, R. W., and B. Droz (1968) The renewal of protein in retinal rods and cones. J. Cell Biol. *39:* 169–184.